to determine the gyromagnetic ratios g_K and g_R. The derived values $g_K=0.49$ and $g_R=0.37$ appear to be in fair agreement with the theoretical values[11,12] $g_K=0.48$, $g_R=0.30$ and 0.32. Also the theoretical values for the reduced $M1$ transition probability, $B(M1, \frac{5}{2}^- \rightarrow \frac{3}{2}^-) = 4.7$ and 3.7, agree with the experimental result.

The magnetic moments and the $B(M1)$ value have also been calculated considering Coriolis admixture of the [510] $K=\frac{1}{2}$ Nilsson state. However, this did not improve the agreement between the observed and calculated values. These calculations were performed with recent Nilsson matrix elements[12] treating g_K as an adjustable parameter.

Upon closer inspection, however, it appears that the mentioned agreement with a pure rotational assignment is quite accidental. This can be seen as follows. If the rotational motion is undisturbed, the second excited state of the $K=\frac{3}{2}$ ground-state band is expected to be at about 170 keV. No level of this energy has been observed.[10] Coulomb excitation experiments[13] indicate that the collective excitations of the ground state have the energies 69.6 and 219.4 keV, deviating strongly from those of a pure rotor. It appears that a more adequate description of these states can only be achieved by resorting to an elaborate bandmixing calculation, probably also including vibrational interactions.

[11] O. Prior, F. Boehm, and S. G. Nilsson, Nucl. Phys. **A110**, 257 (1968).
[12] S. G. Nilsson (private communication).
[13] A. Z. Hrynkiewicz, B. Sawicka, J. Styczén, S. Szymczyk, and M. Szawlowski, Acta Phys. Polon. **31**, 437 (1967); and J. de Boer (private communication).

PHYSICAL REVIEW VOLUME 174, NUMBER 4 20 OCTOBER 1968

Resonant and Nonresonant Capture of Slow Neutrons in $Tm^{169}(n,\gamma)Tm^{170}$†

M. A. Lone,* R. E. Chrien, O. A. Wasson, M. Beer, M. R. Bhat, and H. R. Muether‡
Brookhaven National Laboratory, Upton, New York 11973
(Received 11 June 1968)

The intensities of radiative transitions following slow-neutron capture in $Tm^{169}(n,\gamma)Tm^{170}$ have been measured for neutron energies up to ~136 eV. From the determination of the strengths of transitions feeding final states in Tm^{170}, the partial radiative widths of resonances below 136 eV are determined, and the partial cross sections $\sigma_{n\gamma f}$ below 30 eV are fitted with a simple Breit-Wigner multilevel formula. A direct amplitude is necessary to achieve good fits for several transitions, including that to the ground state. The correlation of the direct amplitude to the strength of the state as observed in (d,p) is investigated.

INTRODUCTION

THE availability of high-resolution radiation detectors and intense neutron sources has made feasible more detailed studies of the radiative de-excitation of states formed in slow-neutron capture. By measuring the decay characteristics of the compound nucleus as a function of the incident neutron energy, it is possible to study the (n,γ) reaction mechanism. By virtue of populating the final states in the residual nucleus, information relating to the nuclear structure of the residual nucleus is obtained.

In this experiment, the partial radiative widths in the reaction $Tm^{169}(n,\gamma)Tm^{170}$ have been measured. The spectra in the "between-resonance" regions have been obtained, and by combining this data with the partial widths of the resonances, multilevel analyses of the partial cross-section ratios in these regions have been performed. The strong interference effects seen in the off-resonance region can only partly be accounted for by interfering levels; a direct amplitude term is necessary to get good fits in general.

Lane and Lynn[1] have discussed the possibility of the direct capture mechanism in the (n,γ) reaction, where an incident s-wave neutron is scattered into a final state without the formation of a compound nucleus. This direct capture can be encompassed by the R-matrix theory by formally identifying it with the faraway levels contribution to the dispersion sum. Similar considerations lead to an entrance channel contribution from the external region.[2] Although this process has the same resonant-energy dependence as the ordinary compound-nucleus contribution, it is proportional to the single-particle component of the capturing state. The channel resonance contribution arises from the part of the dipole integral for which $r \geq R$, and for which the initial wave function may be simply regarded as the target nucleus plus a single neutron. This situation

* State University of New York, Stony Brook, N. Y.; present address: Department of Physics, Indiana University, Bloomington, Ind.
† This work was supported by the U. S. Atomic Energy Commission.
‡ State University of New York, Stony Brook, N. Y.

[1] A. M. Lane and E. Lynn, Nucl. Phys. **17**, 563 (1960); **17**, 586 (1960).
[2] R. G. Thomas, Phys. Rev. **84**, 1061 (1951).

leads to the following relationship between the partial radiation widths $\Gamma_{\lambda\gamma f}$ and the reduced neutron width $\Gamma_{\lambda n}{}^0$:

$$\Gamma_{\lambda\gamma f}=K'S_{fn}\Gamma_{\lambda n}{}^0+\Delta,$$

where K' is a constant, S_{fn} is the reduced neutron width of final state, and Δ includes residual terms, arising from more complex configurations of the target nucleons.

If the channel resonance contributions are strong, the above equation implies that there must be strong correlations between $\Gamma_{\lambda\gamma f}$ and $\Gamma_{\lambda n}{}^0$, and also between $\Gamma_{\lambda\gamma f}$ and S_{fn}. These correlations are a crucial test of the importance of this channel resonance contribution, since otherwise it is indistinguishable from that of the compound-nucleus contribution. So far the efforts to determine experimentally the channel resonance and the direct capture contributions have employed the following three methods:

(1) Comparison between the calculated and the experimental values of the partial and the total cross sections.[1]

(2) Comparison between the (n,γ) and the (d,p) reduced widths.[3]

(3) Determination of the direct capture amplitude from the interference effects between this amplitude and the resonance amplitudes.[4–6]

None of these methods constitutes a completely unambiguous test. Usually there are many competing factors which can make the transition strength of a particular γ ray anomalously strong or weak. Most of the data for (1) and (2) is from the thermal neutron capture. We shall see in the present work that these intensities are in no way characteristic of the average intensities from the resonances. These intensities at thermal energies may be drastically changed by interference between the resonances.[7] Even if the intensities from a few resonances are observed, these may be influenced by the Porter-Thomas distribution,[8] because in the resonances the compound-nucleus contribution (internal region) is usually much more important than the external channel contributions. Thus, unless these effects are taken into account, the correlations or the anticorrelations observed in Refs. 1 and 3 may have little significance.

The third method is the attempt to observe direct capture amplitude between resonances. Earlier work[4] with Na(I) detectors yielded no definite results but recently Wasson *et al.*[5] and Chrien *et al.*[6] using Ge(Li) detectors have been able to establish its existence definitely. In both these cases, the final states showing direct capture have large (d,p) stripping strengths.

Tm^{169} is well suited for applying methods 2 and 3. There are many low-energy resonances and many bound states in Tm^{170} have p-orbital components. Thus, from a knowledge of the partial radiation widths $\Gamma_{\lambda\gamma f}$, we shall be able to determine the correlations between the $\Gamma_{\lambda\gamma f}$ and the reduced neutron widths of the resonances. Several high-energy γ rays are found to be quite strong, thus the direct capture contribution to the states populated by these transitions can be determined by carrying out the interference analysis.

Tm^{170} is a deformed odd-odd nucleus, whose 69th proton configuration is described by the Nilsson orbital $\frac{1}{2}+[411]$ belonging to a $d_{3/2}$ single-particle state. The ground-state neutron configuration is described by the $\frac{1}{2}-[521]$ orbital, belonging to a $p_{3/2}$ single-particle state. From the work of Sheline and his co-workers,[9] it is found that there are five states below an excitation energy of 240 keV with $J\leq 2$, in which the last neutron is in the p orbital.

In the previous studies of $Tm^{169}(n,\gamma)Tm^{170}$ with thermal neutrons, the ground-state transition, although E-1 in character, is found to be very weak. We shall see that this anomalous intensity is explainable in terms of level-level interference. Resonance spins and the level scheme of Tm^{170} will also be examined.

EXPERIMENTAL METHOD

A preliminary account of some aspects of the present work, mainly the correlation between partial widths of $^{169}Tm(n,\gamma)^{170}Tm$, may be found in Ref. 10.

This work was done at the fast chopper facility of the high-flux beam reactor (HFBR) at Brookhaven National Laboratory. This facility has been described earlier by Chrien and Reich.[11] A sample of 192 g of powdered Tm_2O_3 inside an aluminum container, 7×7×1.5 cm, with 0.8-mm walls, was placed at an angle of 45° to the neutron beam at a flight path of 21.7 m; a 10-cc Ge(Li) detector with a resolution of 12 keV at 7 MeV

[3] C. K. Bockelman, Nucl. Phys. **13**, 205 (1959); W. V. Prestwich and R. E. Coté, Phys. Rev. **155**, 1223 (1967); L. V. Groshev and A. M. Demikov, Yadern. Fiz. **4**, 785 (1966) [English transl.: Soviet J. Nucl. Phys. **4**, 558 (1967)]; H. Ikegami and G. T. Emery, Phys. Rev. Letters **13**, 26 (1964); B. B. Kinsey, G. A. Bartholomew, and W. H. Walker, Phys. Rev. **83**, 519 (1951); H. U. Gersch, W. Rudolph, and K. F. Alexander, Nucl. Phys. **54**, 405 (1964).

[4] O. A. Wasson and J. E. Draper, Phys. Letters **6**, 350 (1963); Nucl. Phys. **73**, 499 (1965); D. Dorchoman, B. Kardon, D. Kish, and G. Samosvat, Zh. Eksperim. i Teor. Phys. **46**, 1578 (1964) [English transl.: Soviet Phys.—JETP **19**, 1067 (1964)]; K. J. Wetzel, C. K. Bockelman, and O. A. Wasson, Nucl. Phys. **A92**, 696 (1967); V. D. Huynh, S. de Barros, J. Morgenstern, C. Samour, J. Julien, and G. LePoittevin, *Proceedings of the International Conference on the Study of Nuclear Structure with Neutrons, Antwerp, 1965* (North-Holland Publishing Co., Amsterdam, 1966), p. 551.

[5] O. A. Wasson, M. R. Bhat, R. E. Chrien, M. A. Lone, and M. Beer, Phys. Rev. Letters **17**, 1220 (1966).

[6] R. E. Chrien, D. L. Price, O. A. Wasson, M. R. Bhat, M. A. Lone, and M. Beer, Phys. Letters **25B**, 195 (1967).

[7] R. E. Coté and L. M. Bollinger, Phys. Rev. Letters **6**, 695 (1961).

[8] C. E. Porter and R. G. Thomas, Phys. Rev. **104**, 483 (1956).

[9] R. K. Sheline, C. E. Watson, B. P. Maier, U. Gruber, R. H. Koch, O. B. Shultz, H. T. Motz, E. T. Jurney, G. L. Struble, T. V. Egidy, T. H. Elze, and E. Beiber, Phys. Rev. **143**, 857 (1966).

[10] M. Beer, M. A. Lone, R. E. Chrien, O. A. Wasson, M. R. Bhat, and H. R. Muether, Phys. Rev. Letters **20**, 340 (1968).

[11] R. E. Chrien and M. Reich, Nucl. Instr. Methods **53**, 93 (1967).

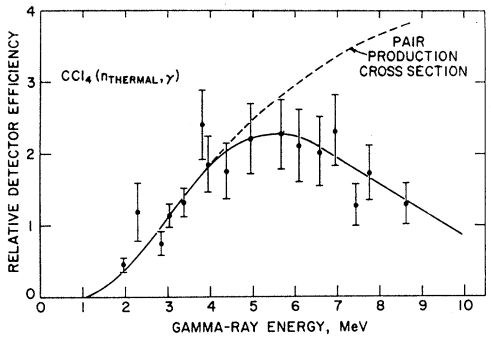

FIG. 1. Relative efficiency for double-escape-peak areas for 10-cc Ge(Li) detector. The intensities for thermal neutron capture in chlorine [L. V. Groskev, A. M. Demidov, V. N. Lutsenko, and V. I. Pelekov, *Atlas of Gamma-Ray Spectra from Radiative Capture of Thermal Neutrons* (Pergamon Press, Inc., New York, 1959)] were used as a basis for this curve.

was used for γ-ray detection. The relative efficiency of the detector, as obtained from an independent experiment with thermal neutrons on a CCl_4 sample, is shown in Fig. 1. Ratios of the full energy to double escape and single-escape to double-escape areas are shown in Fig. 2.

Standard low-noise preamplifiers and amplifiers and a 2048-channel pulse digitizer were used for these measurements. The electronics, other peripheral equipment, and data acquisition methods have been described in detail by Bhat *et al.*[12] The over-all linearity of the electronic system is shown in Fig. 3.

A time-of-flight spectrum taken at 12 000 rpm with 1-μsec channel width and 16-μsec initial electronic delay is shown in Fig. 4. All events which deposit more than 1.56-MeV energy in the detector are included in this spectrum. The error bars under the peaks show the time regions selected for obtaining the pulse-height spectra from these resonances. Small bumps near channels 630, 500, and 300 are due to an Er impurity in the sample and belong to the resonances at 5.98, 9.38, and 26 eV in Er^{167}, respectively. A spectroscopic

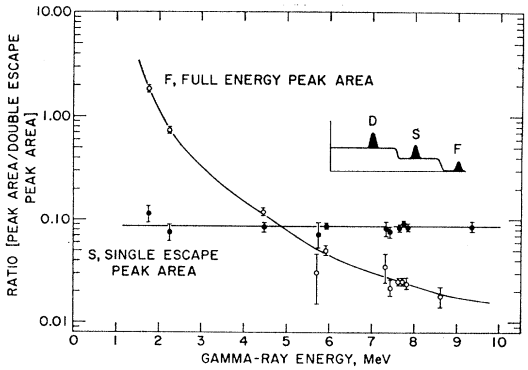

FIG. 2. The ratios of full energy and single-escape-peak area to double-escape-peak area for the 10-cm² Ge(Li) detector used in this experiment.

[12] M. R. Bhat, B. R. Borrill, R. E. Chrien, S. Rankowitz, B. Soucek, and O. A. Wasson, Nucl. Instr. Methods 53, 108 (1967).

analysis of the sample shows that this impurity is less than 0.1%. Other major sources of background include the scattered neutrons off the sample. This background was studied for a general case by Chrien[11] by placing a carbon sample which scattered 98% of the beam at the sample position. A proper thickness of Li^6 or Li_2CO_3 in front of the Ge(Li) detector is sufficient to eliminate most of the scattered neutrons below 100 eV from reaching the detector. For the present experiment, a carbon slab equal in area to the Tm_2O_3 sample and thickness whose scattering is equivalent to potential scattering from the sample was placed in the beam. Normalized time-of-flight spectra for three different samples are shown in Fig. 5. We see from this figure that in this region the background due to scattered events is less than 13%. This is also evident from the peak-to-continuum ratio in the spectrum shown in Fig. 4.

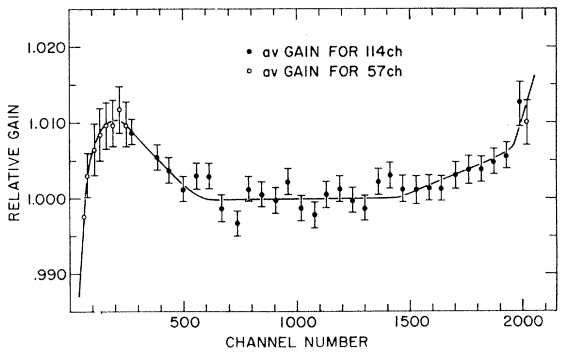

FIG. 3. Linearity of the electronic system.

DETERMINATION OF γ-RAY ENERGIES AND PARTIAL WIDTHS

Figure 6 shows several typical pulse-height spectra, from the resonances at 3.9, 14, 17, and 29 eV. As we shall see later the peaks marked 1, 2, 3, 4, and 5 are of the transitions to the final states of spins 1, 2, 0, 2, and 2. The difference in the appearance of these transitions from the strong resonances at 3.9 and 14 eV reflects the difference in the spins of these resonances. The 17-eV resonance presents an interesting case. All of these transitions except No. 1 are weak, which indicates that the resonance spin might be 0, yet the interference analysis as discussed in the section on nonresonant capture shows that the spin of this resonance is 1. Similar spectra were obtained from other resonances. The changes in the relative intensities of various γ rays from one resonance to another resonance as expected from the Porter-Thomas[8] distribution are clearly visible. The spectrum from the thermal neutron capture is shown in Fig. 7. The complexity of this spectrum is noteworthy. Peaks corresponding to the numbers marked on the channel axes are well resolved in spectra from the resonances. The ground-state

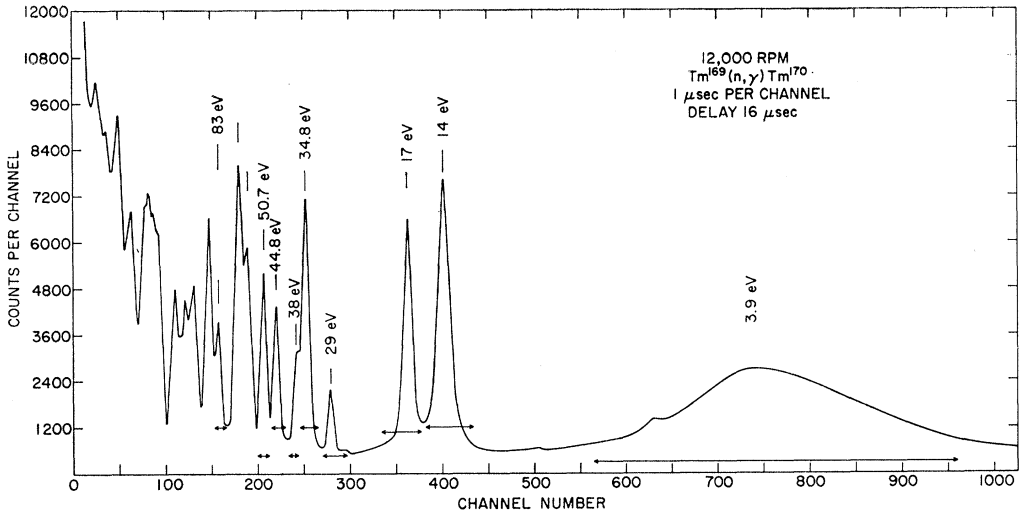

FIG. 4. Time-of-flight spectrum.

transition in this spectrum is very weak, although this is the strongest transition in the 14-eV spectrum. This fact and many other features (discussed later) clearly indicate that the thermal spectrum does not represent a characteristic spectrum from any resonance (although the 3.9-eV resonance dominates in the thermal region) or a good average over all of the capturing states. This difficulty is usually present in interpreting the results of thermal neutron capture.

The peak positions are determined by direct examination of the pulse-height spectra and also with the help of a computer program which can resolve closely spaced peaks. This program makes a skew Gaussian fit to the peak. The function is of the form

$$H\exp[-(x-a)^2(1-\theta b)/2\sigma^2],$$

where $\theta=1$ for $x<a$, $\theta=0$ for $x\geq a$, and a is the position of the peak, H its height, and b the degree of skewness. Any of the variables H, a, b, and σ can be kept fixed or varied.

From Fig. 3 we see that the system is quite linear in the region between 600–1500 channels. In this region, at a gain of 3.774 keV/channel, the integral nonlinearity is 0.21 keV per 100 channels. The error in the γ-ray energy determination due to this nonlinearity is less than the uncertainty in the peak positions due to the statistics. The system gain is obtained from the positions of the single-escape and the double-escape peaks, and the positions of the 6556.4- and the 5945.0-keV γ-ray peaks with the help of the pulser. The γ-ray energy scale is calibrated with respect to the 6556.4- and 5945.0-keV γ rays, taken from the work of Ref. 9. The γ-ray energies are computed from the positions of their respective double-escape-peak positions.

The areas of the two escape peaks of the γ rays are determined in each pulse-height spectrum. The relative peak area of a γ ray f in a spectrum from resonance λ is defined as

$$a_{\lambda\gamma f}=A_{\lambda\gamma f}/A_\lambda,$$

where $A_{\lambda\gamma f}$ is the double-escape-peak area corrected for the detector efficiency. A_λ is the sum of the counts in the whole of the spectrum belonging to the resonance λ. We assume that A_λ is a measure of the neutron capture in the resonances λ; then

$$a_{\lambda\gamma f}=(1/k)(\sigma_{\lambda\gamma f}/\sigma_{\lambda\gamma})=(1/k)(\Gamma_{\lambda\gamma f}/\Gamma_{\lambda\gamma}),$$

where $\sigma_{\lambda\gamma f}$ is the partial capture cross section and $\sigma_{\lambda\gamma}$

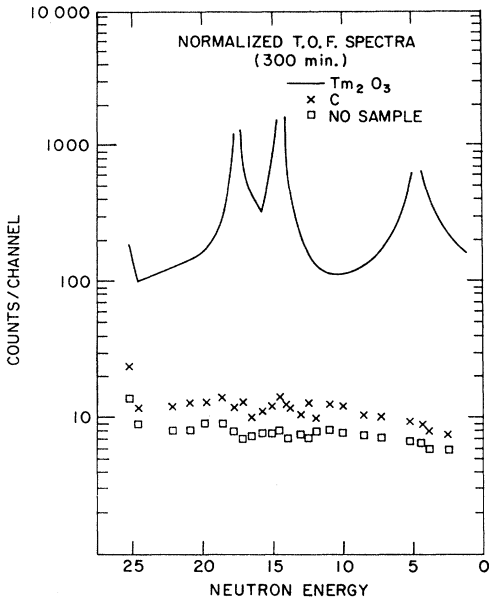

FIG. 5. A comparison of the time-of-flight spectra for the (a) thulium sample, (b) carbon scatterer, and (c) no sample cases. The background contamination of the thulium spectrum is seen to be very small.

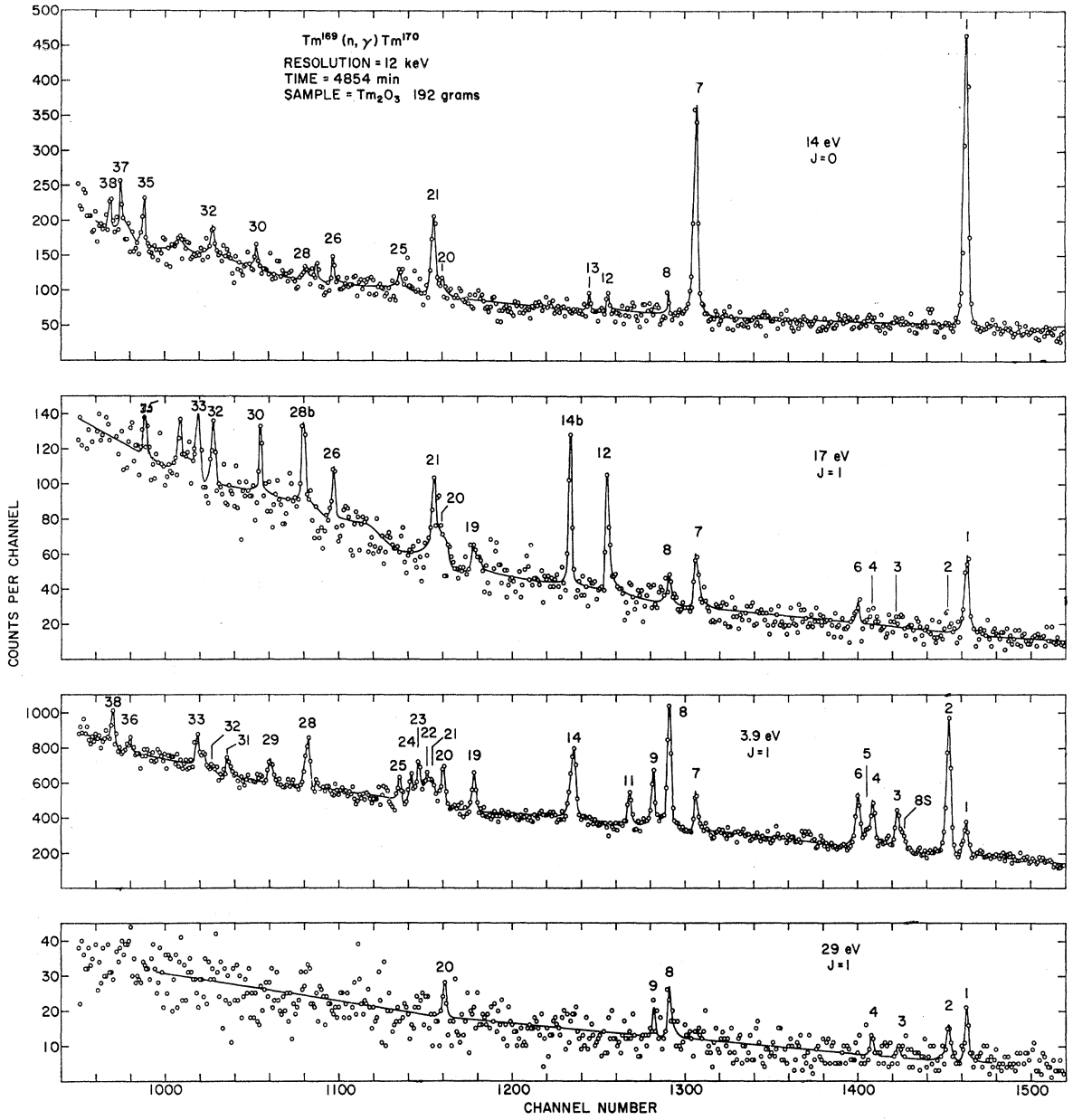

FIG. 6. Pulse-height spectra for 3.9-, 14-, 17-, and 29-eV resonances.

is the total capture cross section. $\Gamma_{\lambda\gamma f}$ and $\Gamma_{\lambda\gamma}$ are the partial radiation width and the total radiation width, respectively, while k is a constant independent of the capturing state. In a spectrum from the thermal neutron capture,

$$a_{\mathrm{th}\gamma f}=(1/k)I_{\mathrm{th}\gamma f},$$

where $I_{\mathrm{th}\gamma f}$ is the intensity per neutron capture of the γ ray f following thermal neutron capture. We use the intensities measured in Ref. 9 to evaluate this constant k. The value of k obtained from the data available on several intense high-energy γ rays from this reference is

$$k=4.0\pm0.34,$$

and the units are such that

$$ka_{\lambda\gamma f}=I_{\lambda\gamma f},$$

where $I_{\lambda\gamma f}$ is equal to the number of primary photons of energy $E_{\lambda f}$ per neutron capture in the resonance λ. The partial radiation width of this γ ray in the resonance λ is then given by

$$\Gamma_{\lambda\gamma f}=I_{\lambda\gamma f}\Gamma_{\lambda\gamma}.$$

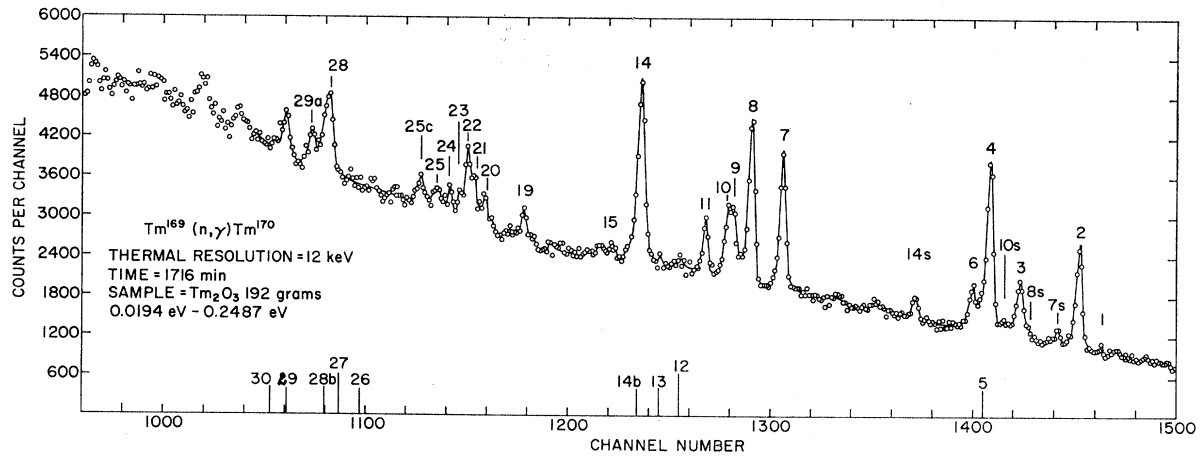

FIG. 7. Pulse-height spectrum from thermal energies.

The energies and the intensities of the primary γ-rays are given in Table I. The uncertainty in the γ-ray energy is ± 3 keV unless otherwise stated. The errors in the intensities are statistical and do not include the systematic error due to k. The upper limits given for some of the high-energy γ rays are equal to twice the standard deviation.

LEVELS OF Tm^{170}

The ground-state spin and parity of Tm^{169} is $\frac{1}{2}^+$. From s-wave neutron capture, states of 0^+ and 1^+ character will be formed. Many of these resonance states can be assigned spins on the basis of observing primary transitions to the final states in Tm^{170}.

Sheline and his co-workers have investigated levels in Tm^{170} by a combination of (d,p) and thermal (n,γ) experiments.[9] Nilsson orbital assignments are given in that reference for all states below 427-keV excitation energy. In the present experiment, we assume that the primary transitions have electric dipole character. These transitions have final-state spins and parities 0^-, 1^-, and 2^-. Below 427 keV all 0^-, 1^-, 2^- states are identified by Sheline as excited neutron configurations.

Table II compares the states excited in the present experiment with those observed by Sheline. The observed transitions in the present experiment are in all cases consistent with the spin assignments proposed by Sheline with the following important exception: Sheline has proposed γ-vibrational states at 411, 456, and 512 keV based on the $K=1^-$ ground-state band, and a state at 662 keV based on the $K=0^-$ band. None of these states are populated in the present experiment, although the dipole selection rules permit populating the proposed 1^- 411-, the 2^- 456-, and the 2^- 662-keV levels.

It is suggested by Sheline *et al.* that the fact that only excited neutron configurations are populated in the (n,γ) reaction indicates the presence of a direct reaction mechanism. We shall present other evidence for a direct mechanism in the section on nonresonant capture.

The spin assignments for the initial states (resonances) can be made by considering the transitions denoted by lines 1, 2, 3, 4, and 5 in Table I. The spins of the final states are 1^-, 2^-, 0^-, 2^-, and 2^-, respectively. The presence of line 3 to the 0^- final state unambiguously fixes the resonance spin as 1^+. The absence, however, of this line does not necessarily indicate a 0^+ resonance, because of the broad distribution of partial radiative widths. All five transitions are allowed from a 1^+ resonance, but only the ground-state line 1 should be observed in a 0^+ resonance. The pulse-height spectra from the $J=1$ 3.9-eV resonance and the $J=0$ 14-eV resonance clearly demonstrate this.

The 14- and 17-eV resonances have spectra which appear to be similar, in the absence of observable transitions to low-lying spin-0 and spin-2 states. However, the interference analysis to be described in Sec. VI clearly demonstrates that the 17-eV resonance has spin 1. This case illustrates the effect of Porter-Thomas fluctuations on making spin assignments based on failure to observe a γ ray allowed by the spin selection rules. The probability that lines 2, 3, 4, and 5 are jointly weaker than the experimental sensitivity has been calculated to be about 20%, based on the χ^2 distribution with one degree of freedom for radiative widths. Thus, the interference analysis is not inconsistent with the observed 17-eV spectrum.

The spin assignments for resonances observed in the present experiment are tabulated in Table III.

STATISTICAL PROPERTIES OF PARTIAL WIDTHS

In Fig. 8 we compare the reduced γ widths of the 11 high-energy γ rays as observed in several resonances. In Fig. 8(a), I_{dp}^{rel} refers to the intensity of the protons observed at a 45° angle. The intensity by itself is not proportional to the reduced width of this final state. (See section on theoretical estimates of direct capture

TABLE I. $I\gamma$ (absolute intensities of the primary transitions, in photons per 1000 captures).[a]

No.	$E_n \rightarrow$ [b] E_γ [c] ↓(keV)	3.92	14.4	17.5	29.1	34.8	38.0	44.8	50.7	(54, 59.2)	(63.0, 65.8)	83.4	(93.5, 94.0)	115	(125, 132, 136)	Thermal
1	6593.9	1.6 ±0.2	17.2 ±0.68	1.2 ±0.3	2.8 ±0.68	0.6 ±0.28	1.3 ±0.76	1.2 ±0.48	1.2 ±0.44	1.5 ±0.32	1.28±0.4	0.17±0.39	1.4 +0.28	.68±0.36	2.1 ±0.44	.21±0.1
2	6556.4±2	7.2 ±0.24	<0.54	0.64±0.22	2.1 ±0.68	0.13±0.23	1.3 ±0.76	1.1 ±0.48	0.0 ±0.32	0.52±0.28	<0.56	1.3 ±0.44	1.3 ±0.32	4.4 ±0.56	0.6 ±0.28	4.9 +0.15
3	6444.9	1.8 ±0.2	<0.56	0.46±0.24	0.3 ±0.59	0.72±0.32	2.9 ±0.96	0.8 ±0.45	0.44±0.44	0.2 ±0.32	<0.62	1.38±0.52	2.0 ±0.32	1.6 ±0.48	<0.84	2.0 ±0.11
4	6389.3	2.2 ±0.2	<0.58	0.29±0.24	1.2 ±0.68	1.8 ±0.38	1.03±0.82	1.7 ±0.6	0.52±0.40	1.2 ±0.36	<0.62	0.39±0.49	1.5 ±0.36	<0.72	<0.86	8.0 ±0.14
5	6375.0	0.96±0.09	<0.56	0.22±0.24	0.59±0.59	1.3 ±0.33	3.7 ±1.0	0.5 ±0.45	0.56±0.44	0.89±0.35	<0.66	0.17±0.44	1.4 ±0.32	<0.94	<0.94	
6	6356.0	2.5 ±0.17	<0.54	0.68±0.26	0.67±0.59	0.92±0.32	2.1 ±0.92	3.8 ±0.62	1.1 ±0.44	1.3 ±0.36	1.7 ±0.4	2.0 ±1.8	<0.76	1.5 ±0.48	2.0 ±0.48	1.9 ±0.12
7	6003.3	1.6 ±0.17	11.2 ±0.58	1.6 ±0.33	0.15±0.74	0.39±0.36	1.0 ±0.9	1.0 ±0.64	0.77±0.48	<0.8	1.6 ±0.44	0.88±0.58	2.3 ±0.48	1.6 ±0.56	<1.16	6.0 ±0.15
8	5944.8	5.5 ±0.22	0.68±0.32	0.92±0.32	2.6 ±0.88	0.86±0.39	4.2 ±1.1	0.0 ±0.5	1.5 ±0.56	1.12±0.47	1.54±0.44	1.5 ±0.64	2.8 ±0.48	1.8 ±0.48	<1.28	7.8 ±0.15
9	5910.8	2.0 ±0.3	0.51±0.22	0.2 ±0.3	1.5 ±0.8	0.49±0.42	0.62±0.92	0.25±0.55	0.44±0.52	<0.78	<0.76	0.0 ±0.61	2.8 ±0.44	1.0 ±0.56	<1.0	3.1 ±0.17
10	5899.5	0.52±0.17	<0.62	0.31±0.31	0.07±0.74	2.9 ±0.48	0.0 ±0.82	0.45±0.55	0.0 ±0.48	<0.84	<0.80	0.0 ±0.55	1.3 ±0.36	<0.86	<1.08	3.2 ±0.15
11	5858.0	1.4 ±0.18	<0.64	<0.62	<1.52	2.7 ±0.48	1.0 ±0.96	3.3 ±0.76	<1.0	1.2 ±0.44	<0.78	<1.22	1.4 ±0.52	1.7 ±0.60	1.0 ±0.56	2.3 ±0.14
12	5809.0	0.0 ±0.16	0.8 ±0.33	3.2 ±0.04	0.0 ±0.74	0.08±0.39	0.0 ±0.82	0.6 ±0.55	0.68±0.56	1.3 ±0.44	9.3 ±0.64	1.2 ±0.68	2.4 ±0.44	1.76±0.6	1.0 ±0.56	
13	5771.2	<0.2	0.68±0.34									0.76±0.6				
14	5736.5	2.7 ±0.24		0.58±0.33	0.9 ±1.6	0.64±0.44	0.8 ±1.6	1.0 ±0.68	0.32∞0.57	1.1 ±0.44		1.1 ±0.64	2.2 ±0.56	2.2 ±0.64		8.8 ±0.17
14*b*	5729.7	1.3 ±0.12		3.5 ±0.46	0.74±0.82	0.29±0.42	0.41±0.92	0.94±0.60	3.3 ±0.64			0.22±0.66			0.92±0.60	
15	5684.4	0.04±0.18	<0.4	0.0 ±0.31	0.0 ±0.74	1.6 ±0.44	1.13±1.03	3.0 +0.76	3.1 ±0.68	2.2 ±0.52		0.22±0.66	1.6 ±0.52	<0.64	2.3 ±0.68	0.6 ±0.15
19	5518.3±6	1.7 ±0.2		0.92±1.2	0.59±0.81	0.72±0.48	0.72±1.13	0.7 ±0.65	0.48±0.64	1.3 ±0.52		0.96±0.72	0.68±0.6	1.3 ±0.9		1.2 ±0.16
20	{5453.1 / 5446.6}	2.0 ±0.21	0.68±0.4	2.4 ±0.72	1.7 ±1.0					1.3 ±0.6			1.7 ±0.6	2.3 ±0.76		0.36±0.16
21	5428±5[d]	1.1 ±0.2												1.3 ±0.72		1.8 ±0.16
22	5416.4	1.9 ±0.24														3.1 ±0.17
23	5397.6	2.1 ±0.21	<0.5													1.8 ±0.18
24	5382.5	1.4 ±0.21	0.75±0.4													0.64±0.22
25	5360.0±6[d]	1.0 ±0.20	1.1 ±0.41			0.52±0.56	0.92±0.84	1.7 ±0.76		1.8 ±0.6				<0.9		0.76±0.19
25*c*	5326.0±6[d]	1.0 ±0.5				2.8 ±0.6				1.0 ±0.56	0.89±0.54					1.4 ±0.46
26	5213.4		0.8 ±0.4	1.5 ±0.48		2.7 ±0.64										
28	5158.7	2.4 ±0.24	0.56±0.44	1.8 ±1.2												6.8 ±0.27
28*b*	5148.5	0.44±0.22		3.0 ±0.56							2.9 ±0.64					
29*a*	5122.1			1.3 ±0.4		0.6 ±0.6										1.9 ±0.2
29	5076.8	1.3 ±0.24														2.1 ±0.16
30	5050.5±5[d]		0.96±0.45	1.5 ±0.56												
31	4982.4	0.76±0.24														
32	4950.4	0.29±0.24	1.2 ±0.5	1.7 ±0.56												
33	4918.3[d]	1.9 ±0.3		1.5 ±0.6							2.2 ±0.7					
35	4801.0		1.8 ±0.6	2.0 ±1.8		1.3 ±1.7										
36	4771.1	0.38±.28									1.1 ±.8					
37	4748.0		1.4 ±0.56													
38	4733.3	1.2 ±0.28	0.84±0.56													
39	4649.6	0.6 ±0.2														
40	4639.0	1.4 ±0.14		0.7 ±0.63		1.5 ±0.8										

[a] Normalized to 12 high-energy γ rays as reported in footnote c below.
[b] Recommended values in eV [*Brookhaven National Laboratory Report No. 325* (U. S. Government Printing Office, Washington, D. C., 1966), 2nd ed., Suppl. 2].
[c] Normalized to line 6556.4 and 5945.0 of energy levels of Tm^{170} [R. K. Sheline *et al.*, Phys. Rev. **143**, 857 (1966)].
[d] Appears to be a doublet.

TABLE II. Levels populated in $Tm^{169}(n,\gamma)Tm^{170}$ and $Tm^{169}(d,p)Tm^{170}$ reactions.

Line No.	Present work E_{ex}(keV) (n,γ)	J^{π}[a]	Sheline *et al.*[b] E_{ex}(keV) (d,p)	J^{π}
1	0.0	1	2.5	1
2	37.5	0, 2	39.5	2
			115.0	
3	149.0	0, 2	149.6	0
			183.3[c]	$4, 3^+$
4	204.6	0, 2	208.2	2
5	218.9	0,2	218.2	2
6	237.9	0, 1, 2	236.6	1
			269.6	3
			353.2	3, 4
			380.4	4
			427.3	
			446.2	3
			542.1	
7	590.6	1	587.8	
			609.9	$1^+, 2^+$
8	649.0	1	650.2	
9	683.1	1	689.6[c]	
10	694.4	0, 2		
			717.9	1^+
11	735.9	0, 2		
			753.9	
12	784.9 ±6	1	787.0	
13	822.7	1		
			841.4	
14	857.4	0, 2		
14b	864.2	0, 2	865.2	
15	909.5	0, 2	915.7	
			985.8	
19	1075.6	0, 2	1069.2	
20	1040.8	0, 1, 2		
	1047.6			
21	1165.9	0, 2	1152.9	
22	1177.3	0, 2		
23	1196.3	0, 2		
24	1211.4	1		
25	1233.9	1		
25c	1267.9	0, 1, 2		
26	1380.5	1		
28	1435.2	1		
28b	1445.4	0, 1, 2		
29a	1471.8	0, 2		
29	1517.1	0, 2		
30	1543.4	1		
31	1611.5	0, 1, 2		
32	1643.5	1		
33	1675.6	0, 1, 2		
35	1792.9	1		
36	1822.8	0, 1, 2		
37	1845.9	1		
38	1860.6	1		
39	1944.3	0 2		
40	1954.9	0, 1, 2		

[a] Parity of all the levels is negative, unless mentioned.
[b] Reference 9.
[c] Appear to be doublets.

cross section.) If all these states were excited by $l_n=1$, then $I_{dp}{}^{45°}$ will be proportional to the reduced width, except for a possible J_f dependence. The Figs. 8(b) through 8(n) give the values of the relative reduced widths $B_{\lambda\gamma f}=B_{\lambda\gamma f}/\sum_f B_{\lambda\gamma f}$, where $B_{\lambda\gamma f}=\Gamma_{\lambda\gamma f}/E_{\gamma f}{}^3$ for several neutron resonances. Distributions of these reduced widths differ from resonance to resonance, as expected from the fact that compound-nucleus formation is the predominant mode of the capture mechanism. In Fig. 8(o), the thermal reduced widths are shown. Figure 8(p) gives the value of the $B_{\lambda\gamma f}$ averaged over 12 spin-1 resonances, whereas Fig. 8(q) gives $B_{\lambda\gamma f}$ averaged over 14 spin-1 and -0 resonances. From the former it is noticeable that there is no systematic dependence of $B_{\lambda\gamma f}$ on the final-state spin. In the latter the reduced width of the final states of spins 0 and 2 are smaller than those of spin 1. This difference stems from the fact that spin-1 final states are populated by E-1 transitions both from spin-1 and spin-0 capturing states, whereas spin-0 and spin-2 final states can be populated from spin-1 resonances only. In fact,

$$\frac{(B_{\gamma f})J_f=1}{(B_{\gamma f})J_f=0,2}=1.54\pm0.15\pm0.31,$$

where $B_{\gamma f}$ is the average over 14 capturing states. Also

$$\frac{(B_{\gamma f})J_f=1}{(B_{\gamma f})J_f=0,2}=1.3\pm0.1\pm0.33,$$

where $B_{\gamma f}$ is the average over 12 spin-1 capturing states. The error (0.1) is due to the experimental uncertainties and (0.33) is the statistical error for a limited sample. The reduced width to a final state depends upon the level spacing at the capturing states as predicted by Blatt and Weisskopf.[13] This is evident from the value of the ratio

$$\frac{\langle B_{\lambda\gamma f}\rangle(J=0)}{\langle B_{\lambda\gamma f}\rangle(J=1)}=2.84\pm0.34.$$

TABLE III. Spin assignment of Tm^{169} resonances.

Resonance—eV	J[a]	J[b]	Present work
3.92	1		1
14.4	0	0	0
17.5	0	1	1[c]
29.1			1
34.8	1	1	1
38.0			1
44.8	1	1	1
50.7	1	1	1
83.4	1	1	1

[a] P. P. Singh (private communication), quoted in *Brookhaven National Laboratory Report No. 325* (U. S. Government Printing Office, Washington, D. C., 1966), 2nd ed., Suppl. 2.
[b] M. Asghar, M. C. Moxon, and C. M. Chaffey, in *Conference on Study of Nuclear Structure with Neutrons* (North-Holland Publishing Co., Amsterdam, 1966).
[c] A preliminary value of 0 for this level is quoted in *Brookhaven National Laboratory Report No. 325* (U. S. Government Printing Office, Washington, D. C., 1966), 2nd ed., Suppl. 2.

[13] J. M. Blatt and V. F. Weisskopf, *Theoretical Nuclear Physics* (John Wiley & Sons, Inc., New York, 1958), p. 648.

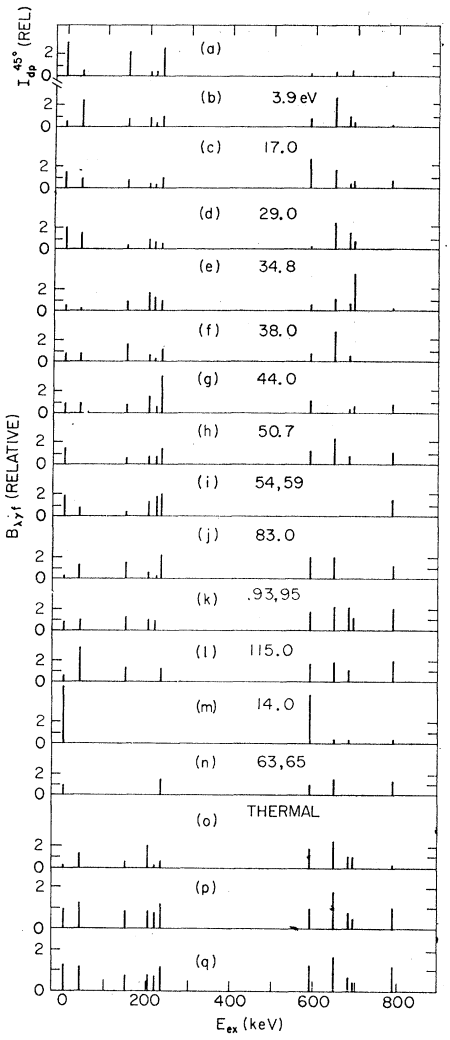

FIG. 8. The relative reduced radiative widths, $B_{\lambda\gamma f} \equiv \Gamma_{\lambda\gamma f}/E_\gamma^3$, for thulium. The d,p intensities at 45° are shown for comparison [Fig. 8(a)].

The error is for a sample size of 10 for the numerator and 165 for the denominator.

Contrary to the lack of knowledge of the final-state reduced widths the reduced neutron widths of the resonances are known. If channel contributions as predicted by Lane and Lynn are present, the reduced partial radiation widths must show a correlation with the reduced neutron widths. Figure 9 shows such a comparison. In the top diagram of this figure, the values of $\Gamma_{\lambda n}^0/\langle\Gamma_{\lambda n}^0\rangle$ are given for various resonances up to 115 eV. Other diagrams give the values of $\Gamma_{\lambda\gamma f}/\langle\Gamma_{\lambda\gamma f}\rangle_\lambda$ for several high-energy γ rays. The γ-ray numbers are the same as in Table I. The correlation coefficient,

$$\rho_f = \frac{\Sigma_\lambda (B_{\lambda\gamma f} - \langle B_{\lambda\gamma f}\rangle)(\Gamma_{\lambda n}^0 - \langle\Gamma_{\lambda n}^0\rangle)}{[\Sigma_\lambda (B_{\lambda\gamma f} - \langle B_{\lambda\gamma f}\rangle)^2 \Sigma_\lambda (\Gamma_{\lambda n}^0 - \langle\Gamma_{\lambda n}^0\rangle)^2]^{1/2}} \left(\frac{N-1}{N}\right),$$

where N is the number of resonances, is given for each line. The correlation coefficient, averaged over final states, is

$$\rho = (1/15)\Sigma_f \rho_f = +0.274.$$

A statistical analysis of the significance of this observed correlation between partial radiative widths and neutron reduced widths of the capturing states has

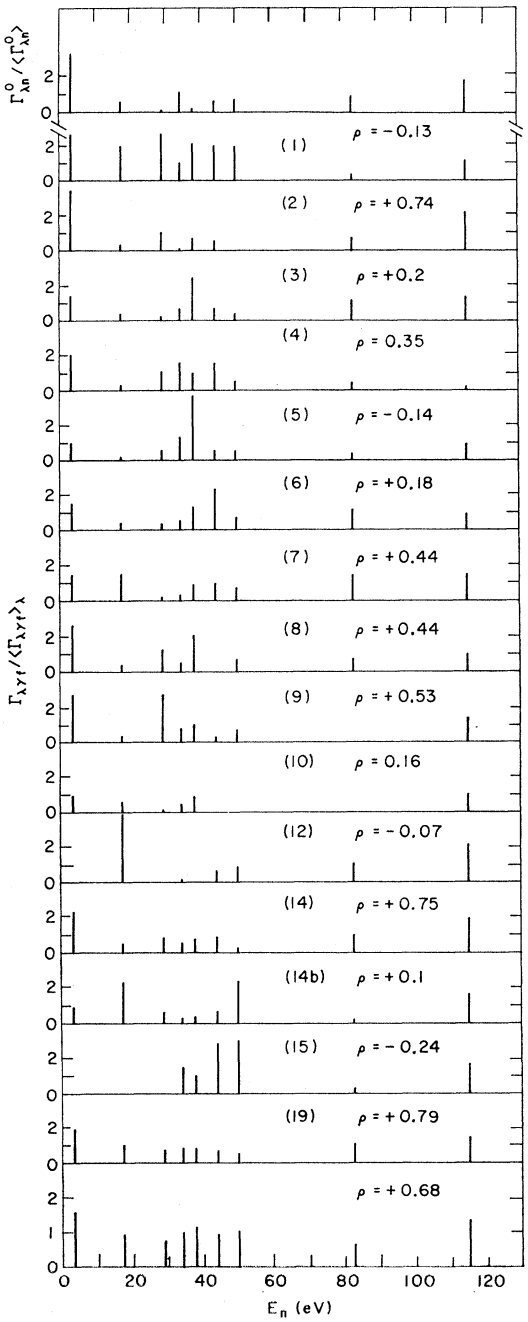

FIG. 9. The relative radiative widths for 9 $J=1$ resonances for 15 final states. The correlation coefficients $\rho_f = \mathrm{corr}(\Gamma_{\lambda n}^0, \Gamma_{\gamma\lambda f})$ are indicated and the relative reduced neutron width is shown.

been published elsewhere.[10] It is shown in Ref. 10 that the probability is less than 1% to obtain a correlation coefficient of 0.274 or higher for an uncorrelated χ^2 distribution with one degree of freedom for the statistical sample composed of eight resonances and 15 final states. There is, then, a negligible probability that the observed correlation is a statistical fluctuation.

Shown in the bottom row of Fig. 9 is the average, over final states, of these 15 transitions. The correlation coefficient of the average width and the neutron reduced width is +0.68. The nonzero value observed in the present experiment may be interpreted as a manifestation of the channel capture hypothesis of Lane and Lynn.[1] The correlation coefficient for each individual transition is also displayed in Fig. 9.

NONRESONANT CAPTURE

Pulse-height spectra for several off-resonance neutron energy regions below 25 eV were obtained and $\sigma_{n\gamma f}/\sigma_{n\gamma}$ determined for these spectra. This ratio is plotted against neutron energy. The background due to the scattered beam was studied by placing a carbon sample of equivalent neutron scattering powder. The normalized time spectra for Tm_2O_3, C, and no sample are shown in Fig. 5. The maximum background contribution at 10 and 25 eV is less than 13%.

A detailed curve fitting has been carried out for 10 of the strongest transitions. We illustrate this procedure by a discussion of several examples. These examples are chosen to be representative of the kinds of fits obtained for these 10 partial cross-section ratios. In several cases equally good fits were obtained by varying the partial width of the bound level, postulated at −4 eV, and altering the relative signs of the product of the reduced width amplitudes for the resonant states, $\sqrt{\Gamma_{n\lambda}^0}\sqrt{\Gamma_{\lambda f\gamma}}$. In other instances, a range of acceptable fits was found within experimental statistics. For these cases, it is not possible to specify an unambiguous value for the direct amplitude parameter D_f^0; a range of D_f^0 values, however, can be specified. In all attempts the same value of D_f^0 for both spin states, $I\pm\frac{1}{2}$, is assumed. Table IV summarizes the partial radiative amplitudes, and their phases, which yielded the best fits to the data. The best-fit curves and discussion are presented below for the 1^- ground-state transition, the 2^- level at 205 keV, and the 1^- level at 591 keV.

Occasionally, an observed partial width was varied within statistical error, to secure a better fit to the experiment.

TABLE IV. Resonance amplitudes for ground, 37.5-, 149-, 204.6-, 237.9-, 590.6-, 649.0-, 683.1-, 735.9-, and 857.4-keV states. Note that the signs shown actually apply to the amplitude product $\sqrt{\Gamma_{n\lambda}^0}\sqrt{\Gamma_{\lambda\gamma}}$. The quantity D, which represents the quantity D_f^0 defined in the text, is dimensionless.

Resonance	J_λ	$E_\gamma=6594$ $D=6\times10^{-5}$	$E_\gamma=6556$ $D=0$	$E_\gamma=6556$ $D=3\times10^{-5}$	$E_\gamma=6444$ $D=0$	$E_\gamma=6444$ $D=6\times10^{-5}$	$E_\gamma=6389$ $D=0$	$E_\gamma=6389$ $D=8\times10^{-5}$
−4.00	1	1.98	4.0	6.0	−0.8	−0.8	−2.8	−3.1
3.92	1	1.19	2.5	2.5	1.32	1.32	1.52	1.44
14.33	0	3.80	0.0	0.0	0.0	0.0	0.0	0.0
17.44	1	0.90	0.6[a]	0.6[a]	0.69[a]	0.69[a]	0.66[a]	0.66[a]
29.10	1	1.50	−1.34	−1.34	−0.84[a]	0.0	−1.0	1.0
34.83	1	0.72	−0.70	0.70	−0.78	0.78	−1.2	1.2
38.00	1	1.02	1.10	−1.10	−1.58	1.58	−1.2	1.2
44.80	1	1.06	−1.0	−1.0	0.0	0.0	−1.32	−1.32
50.70	1	0.97	0.0	0.0	−0.56	0.56	−0.8	−0.8
59.00	1	1.10	−0.64	−0.64	−0.4	0.4	−1.0	0.0
66.00	0	−1.03	0.0	0.0	0.0	0.0	0.0	0.0
93.50	0	−1.10	0.0	0.0	0.0	0.0	0.0	0.0
94.00	1	1.10	−1.0	−1.0	−0.4	0.4	−1.1	0.0
115.00	1	0.79	−0.6	−0.6	−1.2	1.2	−0.8	0.0
130.00	1	1.26	−0.7	−0.7	0.0	0.0	−0.84	0.0
Resonance	J_λ	$E_\gamma=6356$ $D=0$	$E_\gamma=6356$ $D=6\times10^{-5}$	$E_\gamma=6003$ $D=0$	$E_\gamma=5945$ $D=6\times10^{-5}$	$E_\gamma=5911$ $D=0$	$E_\gamma=5858$ $D=0$	$E_\gamma=5736$ $D=0$
−4.00	1	−0.28	−0.48	−1.8	−1.6	−0.80	−0.60	−2.2
3.92	1	1.54	1.54	1.32	2.44	1.54	−1.24	1.98
14.33	0	0.0	0.0	3.28	−0.66	0.66	0.0	0.0
17.44	1	0.88	0.8	1.02	0.99	0.0	0.61	−1.50
29.10	1	0.0	1.0[a]	0.0	−1.51	−1.16	−0.99	−0.88
34.83	1	0.88	0.88	0.0	1.17	−1.17	1.53	−0.74
38.00	1	−1.4	1.4	−0.30	1.94	−0.73	0.95	0.84
44.80	1	−1.9	1.9	−0.30	0.42	−0.46	1.97	−1.4
50.70	1	0.0	0.0	0.0	1.07	−0.90	−0.56	1.68
59.00	1	−1.0	0.0	0.0	0.97	0.0	−1.0	−0.92
66.00	0	1.2	0.0	−1.16	−0.68	0.0	0.0	0.0
93.50	0	0.0	0.0	0.0	0.0	0.0	0.0	0.0
94.00	1	0.0	0.0	−1.40	−1.48	0.0	0.0	0.0
115.00	1	−1.2	0.0	−1.20	−1.26	0.0	0.0	0.0
130.00	1	−0.4	0.0	0.0	0.0	0.0	0.0	0.0

[a] Upper limit.

A. Ground State—$E_{ex}=0$, $E_\gamma=6594$ keV, $J_f^\pi=1^-$

The points in Fig. 10 represent the experimental values of the ratio $\sigma_{n\gamma f}/\sigma_{n\gamma}$. Vertical bars are the statistical errors and the horizontal bars represent the neutron energy region. The arrows on the energy axis show the positions of the resonance. The curves are computed from the formula

$$\frac{\sigma_{n\gamma f}}{\sigma_{n\gamma}}=\sum_J\left|D_f^0+\sum_\lambda\frac{(g_\gamma\Gamma_{\lambda n}{}^0\Gamma_{\lambda\gamma f})^{1/2}}{E-E_\lambda+\frac{1}{2}i\Gamma_\lambda}\right|^2\Bigg/\sum_\lambda\left|\frac{(g_\lambda\Gamma_{\lambda n}{}^0\Gamma_{\lambda\gamma})^{1/2}}{E-E_\lambda+\frac{1}{2}i\Gamma_\lambda}\right|^2,$$

in which it is assumed that all the interference terms in the total capture cross section sum to zero. D_f^0 is the direct or potential capture amplitude for the final state f evaluated at 1 eV. The dotted curve (single level) is calculated by ignoring all interference terms in the partial capture cross section. The discrepancy between the dotted curve and the experimental points indicate the presence of the interference between resonance amplitudes. The data show a destructive interference below the 3.9-eV resonance and a constructive interference above this resonance. Similarly, there is a destructive interference below and a constructive interference above the 14-eV resonance. The strong destructive interference at thermal energy indicates the presence of at least one bound level with spin 1. There is also a discrepancy of (36±10) b between the measured and the calculated value (from the positive energy resonances) of the total cross section at thermal. This discrepancy is only (3±8) b at 1 eV, indicating that the bound state is quite close to thermal energy. Various bound levels with both spins were tried but one near −4 eV with spin 1 gives the best results for the interference analysis and also explains the discrepancy in the total capture cross section. The nature of the interference effects in the 4- to 14-eV region clearly indicates that these resonances have different spins. Similarly, constructive interference on the high-energy side of both the resonances at 14 and 17 eV indicates that these resonances do not interfere and their spins are different. Thus, the 17- and 3.9-eV resonances have the same spin. This conclusion is reinforced by the interference analyses for the other γ-ray transitions. The solid curve is obtained by including all the cross terms in the preceding equation. The resonance amplitudes and their phases are given in Table IV. The amplitudes of positive energy resonances (up to 130 eV) are calculated from the measured partial radiation widths of these resonances. The direct capture cross section for the ground state at 1 eV is

$$\sigma^D(1\text{ eV})=2.3\text{ mb}.$$

Sheline has assigned the ground state as the $K=1^-$ bandhead of the $p\frac{1}{2}^-[411\downarrow]$; $n\frac{1}{2}^-[521\downarrow]$ configuration. It is strongly fed in the (d,p) reaction.

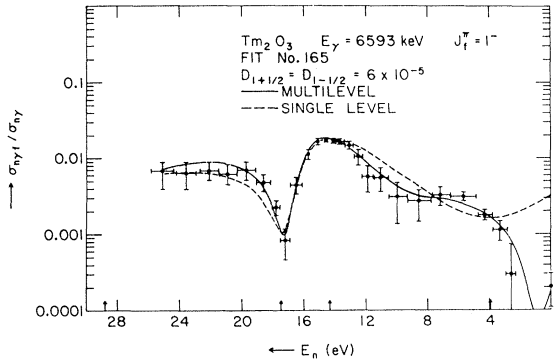

FIG. 10. $\sigma_{n\gamma f}/\sigma_{n\gamma}$ curve for ground state.

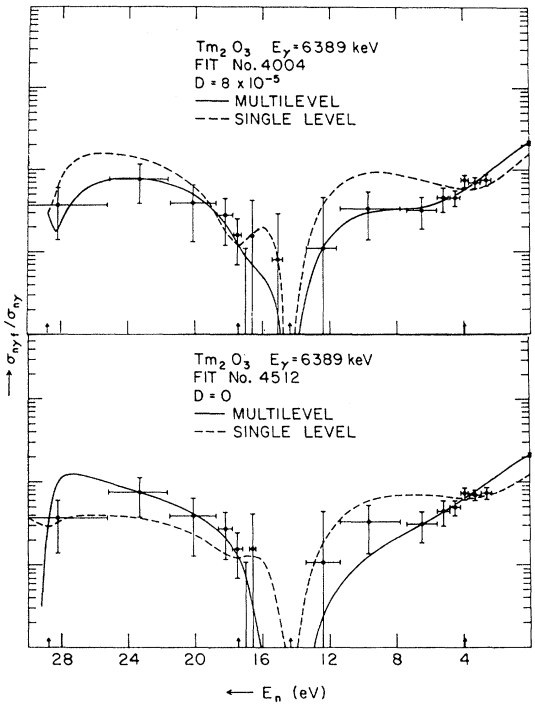

FIG. 11. $\sigma_{n\gamma f}/\sigma_{n\gamma}$ curve for 204.6-keV state.

B. γ Ray No. 4—$E_{ex}=205$ keV, $E_\gamma=6389$ keV, $J^\pi=2^-$

The transition to this state shows a constructive interference at thermal energies, as is shown in Fig. 11. But the nature of such an effect above the 17.4-eV resonance is not clear. For the fit (4004) the curves are calculated by assuming a nonzero value of the direct amplitude which produces destructive interference above the 17.4-eV resonance. On the other hand, curves for the fit (4512) are calculated by assuming a zero value of the direct amplitude which yields constructive interference in the same region. Both the curves seem to fit the data equally well. The amplitudes are given in Table IV. The limits on the direct capture amplitude D_f^0 are

$$0\leq D_f^0\leq 8\times10^{-5}.$$

This state is identified in Ref. 9 as the $K=2$, 2^- state with the neutron in the $\frac{5}{2}$-[512↑] configuration. It is weakly fed in the (d,p) reaction.

C. γ-Ray Peak No. 7—$E_{ex}=591$ keV, $E_\gamma=6003$ keV, $J^\pi=1^-$

The transition to this state shows a strong constructive interference at thermal energies, as is shown in Fig. 12. The solid curve obtained with $D_f{}^0=0$ fits the data quite well. The curves calculated with nonzero $D_f{}^0$ do not fit the data. The resonance amplitudes are given in Table IV. It is concluded that for this γ ray

$$D_f{}^0=0.$$

The existence of this state in the d, p data is described as doubtful.[9] It has not been assigned an orbital configuration in the analysis of Sheline.

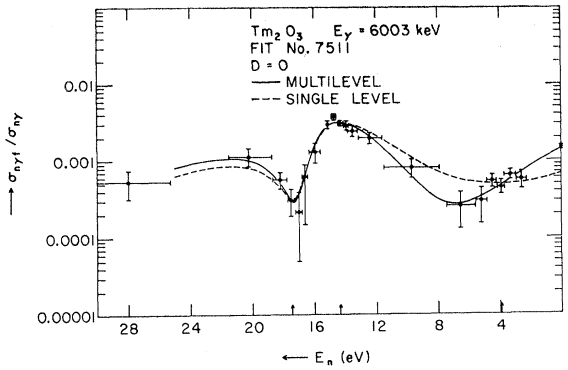

FIG. 12. $\sigma_{n\gamma f}/\sigma_{n\gamma}$ curve for 590.6-keV state.

THEORETICAL ESTIMATES OF DIRECT CAPTURE CROSS SECTION

The cross section for the direct capture of a neutron to a final state of spin, J_f, assuming hard-sphere scattering, is given in Ref. 1 as

$$\sigma_f{}^D=g_f\frac{0.062}{R\sqrt{E_n}}\left|\frac{Z}{A}\right|^2\theta_f{}^2y^2\left(\frac{y+3}{y+1}\right)^3\text{b},$$

where E_n is the neutron energy in eV, g_f is the statistical factor given by

$$g_f=[\textstyle\sum s'(2J_f+1)]/6(2I+1),$$

where I is the spin of the target nucleus and the number of terms in this summation is equal to the number of channel spins s' which satisfy the relationship

$$J_f=s'+l_f,$$

where l_f is the orbital angular momentum of the final state. For Tm^{170} at 1-eV energy,

$$\sigma^D=(0.00127)g_f\theta_f{}^2y^2[(y+3)/(y+1)]^2\text{b},$$

where y^2 is a dimensionless quantity and is equal to $k_{Nl}{}^2R^2$ and k_{Nl} is the wave number corresponding to the binding energy E_{Nl} of a nucleon state $|N_l\rangle$. The quantity E_{Nl} is approximately equal to $E_{\gamma f}$, the energy of the γ-ray transition which populates the final state, while $\theta_f{}^2$ is the reduced width of the final state and is unity for a pure single-particle state. In Table V calculated and experimental values of the direct capture cross section for 1-eV neutrons are compared. The calculated values in column 6 are in units of $\theta_f{}^2$. Noting that the maximum value of $\theta_f{}^2=1$, we see that the experimental values are not inconsistent with the calculated values.

In principle, $\theta_f{}^2$ can be obtained from the $Tm^{169}(d,p)$-Tm^{170} reaction. The differential cross section or the intensity of the proton groups observed at a fixed angle in such an experiment is given by[14]

$$I_{d,p}{}^\theta=kd\sigma/d\omega,$$

$$d\sigma/d\omega=(2J_f+1)/(2J_i+1)\{\textstyle\sum_l S_l\varphi_l(\theta)\},$$

$$S_l=\textstyle\sum_j\theta_{jl}{}^2,$$

where J_f, J_i represent the residual state and target nucleus spins, respectively, φ_l the intrinsic single-

TABLE V. The direct capture cross section $\sigma_f{}^D$. The bracketed numbers are tentative. The line number corresponds to Table I.

Line No.	E_γ(MeV)	E_{ex}(keV)	$J_f{}^\pi$[a]	l_f[a]	Lane-Lynn $\sigma^D(1\text{ eV})\times\theta_N{}^2$ (mb)	$I^{45°}(d,p)$	Expt. $\sigma^D(1\text{ eV})$ (mb)
1	6.5939	0.0	1^-	1	15.5	1.0	2.3
2	6.5564	37.5	2^-	(1, 3)	13.0	0.15±0.04	0–0.6
3	6.4449	149.0	0^-	1	3.0	0.68±0.09	0–2.3
4	6.3893	204.6	2^-	(1, 3)	13.0	0.1 ±0.06	0–4.2
6	6.3560	237.9	1^-	1	15.5	0.86±0.09	0–2.3
7	6.0033	590.6	1^-	1	15.5	0.04±0.02	0.0
8	5.9448	649.1	(1^-)	(1)	15.5	0.23±0.04	2.3
9	5.9108	683.1	(1^-)	(1)	15.5	0.13±0.04	0.0
11	5.8580	735.0	$(0^-, 2^-)$	(1, 3)	3–13.0		0.0
14	5.7365	857.4	$(0^-, 2^-)$	(1, 3)	3.0–13.0		0.0

[a] The bracketed numbers are tentative.

[14] G. R. Satchler, Ann. Phys. (N. Y.) 3, 275 (1958).

particle cross section, and S_l the spectroscopic factor, containing the nuclear structure information.

Satchler[14] has calculated the θ_{jl}, or reduced width amplitude, for a deformed rotating nucleus, in terms of the Nilsson quantum numbers K and Ω. The expression for θ_{jl} is the following:

$$\theta_{jl}(K_i\Omega_i,K_f\Omega_f)=g[(2J_i+1)/(2J_f+1)]^{1/2}\langle J_fK_f|J_ij \pm K_i\Omega_f\pm\Omega_i\rangle\langle\varphi_f|\varphi_i\rangle C_{jl}(\Omega_f\pm\Omega_i).$$

The Clebsch-Gordan coefficient represents the probability of finding the incident neutron and target nucleus in correct alignment for nucleon transfer, while the C_{jl} expansion coefficient represents the fraction of the spherical state Y_{jl} contained in the intrinsic Nilsson orbital. The effect of the overlap factor $\langle\varphi_f|\varphi_i\rangle$ for the vibrational components is not important for low-lying excitations.

For odd-odd residual nuclei like Tm^{170}, various values of l may contribute to each final state, as can be seen from the above equation.

Actual measurements of the angular distributions in Ref. 9 suggest that for the final states 1, 2, 3, and 6 in Table V, l_n is 1, although the $l=1$ and $l=3$ distributions are not very different. These and all other states reported in this table are of negative parity and hence can only be excited with $l_n=1$ or $3(J_f\leq 2)$ in the (d,p) reaction. If the final-state spin is 1, l_n must be 1. But if the final-state spin is 2, l_n can be 1 or 3. Presence of the primary transitions to the states numbered 7, 8, and 9 from the zero-spin resonances indicates that the spin of each of these states is 1, thus l_n is also 1. The spin of the final state 4 is 2 and no definite assignment of the l_n can be made. Similarly, l_n can be either 1 or 3 for the states 11 and 14, since their spins are unknown.

Table V shows a comparison between the $I_{dp}^{45°}$ of a final state relative to the ground state and the direct capture cross section for the same final state. For the states numbered 2, 7, 9, 11, and 14 a small or zero value of $I_{dp}^{45°}$ is associated with a small or zero value of D^2. On the other hand, for the states 1, 3, and 6 a large value of $I_{dp}^{45°}$ is associated with a large value of D^2, although in case of 3 and 6 no definite commitment can be made. In case of the state 4, a small value of the relative width of the final state could be due to an incorrect l_n assignment. If l_n for this state is 3 instead of 1 the reduced width will be much larger. The final state 8 is the only state which shows a reverse trend. The fits obtained for this γ ray are not very satisfactory. It is difficult to say whether the lack of the correlation in this case is due to the poor fit or some other reasons. The balance of the evidence indicates that final states with large $l=1$ components can be associated with nonzero values of the direct amplitude.

CONCLUSIONS

In this work we have measured the energies and the partial radiation widths of many primary γ-ray transitions following neutron capture in several resonances. The average intensities, i.e., averaged over capturing states of the same spin, show no marked dependence on the final-state spin. On the other hand, the average intensity to a given final state show strong dependence upon the level spacing at the capturing states as predicted by Blatt and Weisskopf. From the interference effects between the resonance amplitudes for a particular final state and the strength of the primary transitions to final states of known spin, the spins of several resonances have been determined. The final states up to 400 keV populated by the primary transitions are consistent with the level scheme proposed by Sheline *et al.*,[9] except that there seems to be no evidence for the γ vibrational bands proposed in this reference. A nonzero, positive correlation between the partial radiation widths and the reduced neutron widths is observed in this experiment. This is interpreted as the "channel capture" suggested by Lane and Lynn. The nonzero direct amplitudes necessary to fit the neutron energy dependence for partial cross sections for transitions feeding states with strong $l=1$ components confirm the importance of the direct mechanism in the (n,γ) reaction.